Technical Paper

A Wind Generated Wave Prediction System in a Finite Depth Sea+

Sun H. Kwon*

(*Received November* 9, 1989)

바람에 의해 생성된 파도의 예측과 깊이변화의 영향

권 순 홍*

Key Words : Ocean Wave Model(해양파 모델), Wave Spectrum(파 스펙트럼), Wave Prediction(파고 예측), Wave Refraction(파 굴절)

초 록

해양에서 바람에 의해 생성된 파도를 예측하는 모델을 제시하고 이 모델의 성질을 무한 해면에서 나타내 보이고 마지막으로 파의 이송과 깊이의 영향에 관한 결과를 유한 폭의 해상에서 계산해서 비교 가능한 자료와 비교해 보았다.

1. Introduction

Since the pioneering paper of Phillips[1], wave prediction theories have been applied to the wave forecasting. A lot of researches have been done on the development of numerical wave models. Wave hindcasting models are in use today to get regional wave statistics. Wave forecasting models are in operation now around the world. But most models perform with varing degrees of accuracy, further researches should be done on them.

In this study, a proposed numerical wave model is introduced. The proposed wave model, VPINK, was developed by Neu and Kwon[2,3,4]. VPINK is a decoupled propagation wave model. Calculations are made for the cases of a stationary wind, early growth of wave, the relaxation of a fully developed spectrum under a sudden change of wind direction without a change in wind speed for an infinite ocean. A propagation scheme is then added to examine the case of finite region. Finally the refraction scheme is introduced to take care of the depth effects on waves. The method is applied to the case of wave refraction occurring at a spherical shoal with a diameter of 40*m* and water depth of 5*m* at its top, set in water of uniform depth 15*m*. The distribution of wave energy is calculated.

+ Presented at the 1989 KCORE Autumn Conference(Nov., 1989)

* Member, Dep't, of Naval Architecture, Pusan National University

2. Formulation of the deep water model

VPINK is a decoupled propagation wave model, suitable for a finite ocean applications. Only a short description of VPINK will be given here. VPINK starts from a version of the energy balance equation (Hasselmann)[5],

$$\frac{\partial E(f,\theta;\vec{x},t)}{\partial t} + \nabla \cdot (\vec{C}_g E) + \partial\{(\vec{C}_g \cdot \nabla\theta)E\}/\partial\theta$$

$$= S(f,\theta;\vec{x},t) = S_{in} + S_{nl} + S_{ds} \cdots\cdots\cdots (2.1)$$

where E is the two dimensional directional frequency wave spectrum being a function of position $\vec{x}$, time t, wave frequency f, and direction of propagation θ. $\vec{C}_g$ is the group velocity of the spectral component and S represents the sum of individual source functions. S_{in}, S_{nl}, and S_{ds} represent the wind input, nonlinear wave interaction and dissipation source functions respectively. The nonlinear wave-wave interaction is neglected in this study. The energy input from the wind S_{in} is represented as

$$S_{in} = A(u,f,\alpha) + B(u^*,f,\alpha)E(f,\theta,\vec{x},t) \cdots (2.2)$$

where u is the wind speed. u^* is the friction velocity and α is the angle between wind and wave directions. The A (u,f,α) term is based on the theory of phillips[10]. Phillips mechanism represents the generation of waves on an initially calm water surface through the turbulent atmospheric pressure fluctuations. A form of the A term is adopted

$$A(f,u_{6.1},\alpha) = A_1(f,u_{6.1},\alpha) \quad \text{if} \quad \frac{\omega}{u_{6.1}} \leq 0.02 \cdots\cdots (2.3)$$

$$A(f,u_{6.1},\alpha) = A_1(f,u_{6.1},\alpha) \quad \text{if} \quad \frac{\omega}{u_{6.1}} > 0.02 \cdots\cdots (2.4)$$

where

$$A_1(f,u_{6.1},\alpha) = \frac{4.73\times10^{-16}\omega^4 u_{6.1}^3}{Q_1(\omega,u_{6.1},\alpha)R_1(\omega,u_{6.1},\alpha)} \cdots\cdots (2.5)$$

$$A_2(f,u_{6.1},\alpha) = \frac{7.167\times10^{-14}\omega^{5.25}u_{6.1}^{1.75}}{Q_2(\omega,u_{6.1},\alpha)R_2(\omega,u_{6.1},\alpha)} \cdots\cdots (2.6)$$

and

$$Q_1 = 0.2704\left(\frac{\omega}{u_{6.1}}\right)^2 + \left(\frac{\omega^2}{g}\sin\theta\right)^2 \cdots (2.7)$$

$$Q_2 = Q_1 \cdots\cdots (2.8)$$

$$R_1 = 4.87\times10^{-6} + \left(\frac{\omega^2}{g}\cos\theta - \frac{\omega}{u_{6.1}}\right)^2 \cdots (2.9)$$

$$R_2 = 0.1089\left(\frac{\omega^2}{g}\right)^{2.5} + \left(\frac{\omega^2}{g}\cos\theta - \frac{\omega}{u_{6.1}}\right)^2 \cdots (2.10)$$

A_1 and A_2 are in m^2/rad, $u_{6.1}$ wind velocity at 6.1 m above the water surface is in m/s^2. The $B(u^*, f,\alpha)E(f,\theta;t)$ term is the result of the interaction of the air flow with the already disturbed water surface. Miles[6,7,8,9] considered the perturbation of the mean shear flow in the air by the disturbed water surface, but he neglected the effects of atmospheric turbulence. Pillips[10] extended the analysis to consider the interaction of the wave induced air flow perturbation with the free stream turbulence. The proposed final form of the B term is given

$$\frac{B}{f} = \frac{\rho_a}{\rho_w C^2 K}\left\{\frac{M^n N^2 K^4}{\cos^2\alpha}\left(\frac{-U''}{(U')^3}\right)_{zm}\left(\int_{zm}^{\infty}[U(z)\cos\alpha - C]^2 e^{-kz}dz\right)^2 + M\int_0^{\infty} N^2(-U'')\cos\alpha \, |U\cos - c| \, e^{-2kz}\, dz\right\} \cdots\cdots (2.11)$$

where the mean wind profile can be written as

$$U = \frac{u^*}{k}\ln\left(\frac{z}{z_0}\right) \cdots\cdots (2.12)$$

k is Von Karman's constant and z_0 is the roughness height. In this study Wu's expression is adopted as

$$z_0 = 0.112\frac{(u^*)^2}{g} \cdots\cdots (2.13)$$

z_m is the matched layer height where the wind velocity matches the phase velocity of the wave. z_0 can be related with z_m as

$$z_0 = z_m \exp\left[\frac{-kc}{u^*\cos\alpha}\right] \cdots\cdots (2.14)$$

$M_m = \pi$, $M = 1.6\times10^{-2}$, $N^2 = 1/3$, for $z > z_m$, $N^2 = 1$ for $z < z_m$

VPINK model prevents the wave spectrum from growing above an assumed fully developed limit by balancing the input from the wind with the dissipation without explicitly modeling the dissipation for waves travelling with the wind. Due to the structure of the model, a limiting directional wave spectrum must be assumed as a function of wind speed. The form used here is the Pierson-Moskowitz[11] spectrum with spreading function, which was derived by SWOP project (Cote, et al.)[12]. The fully developed spectrum is thus $E_\infty(\omega,\alpha,u) = E_\infty(\omega, u)\ F(\omega, \alpha, u)$ where

$$E_\infty(\omega,u) = \gamma\ g^2\ \omega^{-5}\ \exp\ [-(\beta(\omega_0/\omega)^4)] \quad \cdots\cdots (2.15)$$

where $\omega=2\pi f$, $\omega_0=g/u$, u being the mean wind speed measured at 19.5*m* above the sea surface $\gamma=8.1\times10^{-3}$ and $\beta=0.074$.

3. Propagation Scheme

For a finite ocean, second term in the left hand side of Equation (2.1) is nonzero and must be modeled by a propagation scheme. A modified Lax-Wendroff scheme due to Gadd[13-15] is used to propagate the wave energy in two dimensions. This scheme was originally applied by Gadd to numerical weather prediction and was first applied to ocean waves by Golding(1983). For one dimensional propagation at speed c, the finite difference expression is represented as

$$E^{n+1/2}_{j+1/2} = \frac{1}{2}(E^n_j + E^n_{j-1}) - \frac{1}{2}\mu(E^n_{j+1} + E^n_j) \quad \cdots\cdots (3.1)$$

$$E^{n+1/2}_j = E^n_j - \mu\{(1+q)(E^{n+1/2}_{j+1} - E^{n+1/2}_{j-1}) - \frac{q}{3}(E^{n+1/2}_{j+3/2} - E^{n+1/2}_{j-3/2})\} \quad \cdots\cdots (3.2)$$

where

$$\sigma = c\frac{\Delta t}{\Delta x}, \qquad q = \frac{3}{4}(1-\sigma^2) \quad \cdots\cdots (3.3)$$

j signifies spacial position and n the time level. For points one grid length from a boundary, q is set to zero. Along the boundary, upstream differences are used for outflow components while inflow values are specified. For two dimensional propagation, the scheme takes the form

$$E^{n+1/2}_{i+1/2,j+1/2} = 1/4(E^n_{i+1,j+1} + E^n_{i+1,j} + E^n_{i,j+1} + E^n_{i,j}) - 1/4\{\sigma[E^n_{i+1,j+1} + E^n_{i+1,j} - E^n_{i,j+1} - E^n_{i,j}] + \varepsilon[E^n_{i+1,j+1} + E^n_{i,j+1} - E^n_{i+1,j} - E^n_{i,j}]\} \quad \cdots\cdots (3.4)$$

$$\begin{aligned} E^{n+1}_{i,j} = E^n_{i,j} - \frac{(1+q)}{2}&\{\sigma[E^{n+1/2}_{i+1/2,j+1/2} + E^{n+1/2}_{i+1/2,j-1/2} - E^{n+1/2}_{i-1/2,j+1/2} - E^{n+1/2}_{i-1/2,j-1/2}]\ \varepsilon[E^{n+1/2}_{i+1/2,j+1/2} \\ &+ E^{n+1/2}_{i-1/2,j+1/2} - E^{n+1/2}_{i+1/2,j-1/2} - E^{n+1/2}_{i-1/2,j-1/2}]\} \\ &+ \frac{q}{9}\{\sigma[E^{n+1/2}_{i+3/2,j+1/2} + E^{n+1/2}_{i+3/2,j-1/2} - E^{n+1/2}_{i-3/2,j+1/2} - E^{n+1/2}_{i-3/2,j-1/2}]\ \varepsilon[E^{n+1/2}_{i+1/2,j+3/2} + \\ &E^{n+1/2}_{i-1/2,j+3/2} - E^{n+1/2}_{i+1/2,j+3/2} - E^{n+1/2}_{i-3/2,j-3/2}]\} \\ &+ \frac{q}{18}\{\sigma[E^{n+1/2}_{i-3/2,j+3/2} + E^{n+1/2}_{i+3/2,j-3/2} - \\ &E^{n+1/2}_{i-3/2,j+3/2} - E^{n+1/2}_{i-3/2,j-3/2}]\ \varepsilon[E^{n+1/2}_{i+3/2,j+3/2} + \\ &E^{n+1/2}_{i-3/2,j+3/2} - E^{n+1/2}_{i+3/2,j+3/2} - E^{n+1/2}_{i-3/2,j-3/2}]\} \quad \cdots\cdots (3.5) \end{aligned}$$

$$\sigma = c\ \cos\theta\frac{\Delta t}{\Delta t},\ \varepsilon = c\ \sin\theta\frac{\Delta t}{\Delta y}\ \cdot\ q = \frac{3}{4}(1-\lambda^2)$$

$$\lambda^2 = \sigma^2 + \varepsilon^2 \quad \cdots\cdots (3.6)$$

where θ is the direction of propagation and $\lambda^2 \leq 1$ is the stability criterion for the two-dimensional scheme.

4. Refraction Scheme

The refraction scheme is due to Golding[16]. It is simply based on a Snell's law.

$$\frac{\partial(k\sin\alpha)}{\partial s} = 0 \quad \cdots\cdots (4.1)$$

where s is a ray path, k is the wave number and α is the angle between s and the depth gradient. α can be expressed in terms of θ, and ∇H, the depth gradient, then Eq.(4.1) may be expressed as

$$\frac{\partial\theta}{\partial s} = -\left\{\left(\frac{\partial H}{\partial x}\sin\theta - \frac{\partial H}{\partial y}\cos\theta\right)\Big/\left(\frac{\partial H}{\partial x}\right.\right.$$

$$\cos\theta + \frac{\partial H}{\partial y}\sin\theta\Big)\Big\}\left\{\frac{1}{k}\frac{\partial k}{\partial s}\right\} \cdots (4.2)$$

Differentiation of dispersion relation gives rise to

$$\partial k/\partial s = -\{k^2 \mathrm{sech}^2 KH/(\tanh kH + kH\ \mathrm{sech}^2 kH)\}\ \{\partial H/\partial s\} \cdots\cdots\cdots (4.3)$$

Combining this equation with (4.2) gives

$$c_g \cdot \nabla\theta = -\mid C_g \mid /k\left(\frac{\partial H}{\partial x}\sin\theta - \frac{\partial H}{\partial y}\cos\theta\right)$$
$$\{-k^2 \mathrm{secH}^2 kH/(\mathrm{than}\ \ kH + kH\ \ \mathrm{sech}^2\ kH\} \cdots\cdots\cdots (4.4)$$

Once we get $C_g \cdot \nabla\theta$, the refraction can be obtained from

$$\partial E_{i,j}/\ \ \partial t = -\partial\{(C_g \cdot \nabla\theta)E_{i,j}\}/\partial\theta \cdots (4.5)$$

The right hand side is calculated using a form of upstream difference in θ.

5. Numerical applications and results

The first case presented is that of wave growth on an initially calm sea under the influence of a steady wind. The results from VPINK are given in Figures 1, 2, and 3. Computations were performed for 40 *knot* wind speed. A three hour time steps was used. The spectral components near the wind direction reach saturation while those

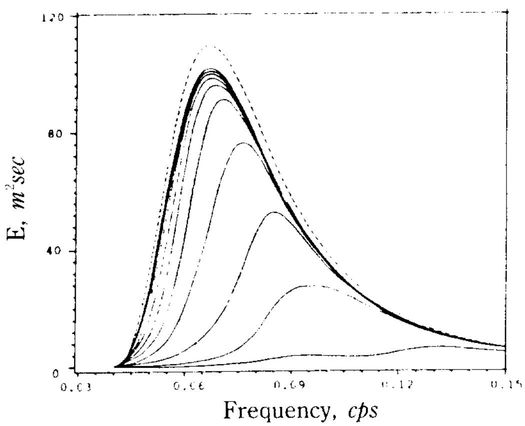

Fig. 1 Point spectrum evolution for a steady 40 *knot* wind in 3 *hour* time increment

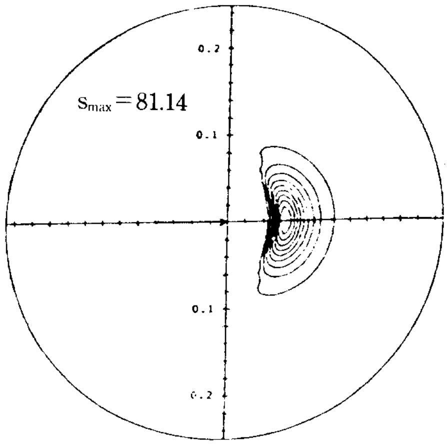

Fig. 2 Contour plot of 2−D spectrum evolution for a steady 40 *knot* wind. T=30*hours*

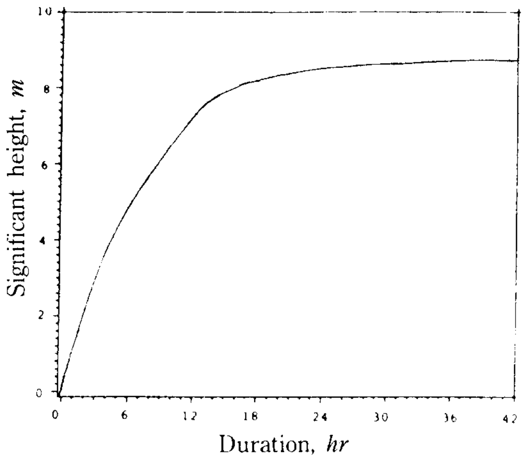

Fig. 3 Significant wave height vs. duration for a steady 40 *knot* wind

away from the wind are still growing at a slow rate. Figure 3 shows significant wave height predicted by the model.

Early wave growth is considered again by taking a 40 *knot* wind blowing over an initially calm sea but with a time step of 0.2 *hours*. Figure 4 shows the directional spectrum. These figures clearly show a bimodal spectrum due to the A term growth maximum near f=0.09*Hz* and the B

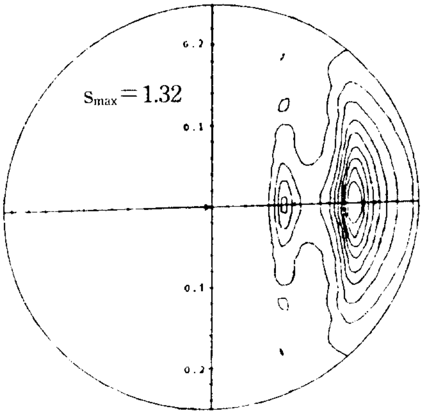

Fig. 4 Contour plot of 2−D spectrum evolution for a 40 *knot* wind at early T=1 *hour*

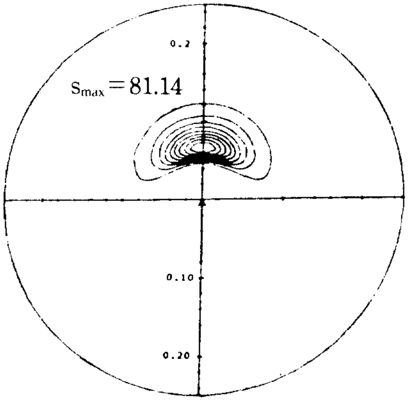

Fig. 5 Initial condition for 90° change of wind direction

term spectral peak. Figure 4 also shows the A term resonance mechanism as predicted by Phillips. The resonance mechanism predicts maximum wave growth when

$$u \cos\alpha = c \quad \cdots\cdots\cdots\cdots\cdots\cdots\cdots\cdots\cdots\cdots\cdots \quad (5.1)$$

or for deep water

$$f \cos\alpha = \frac{g}{2\pi u} \quad \cdots\cdots\cdots\cdots\cdots\cdots\cdots\cdots\cdots \quad (5.2)$$

since $c = g/2\pi f$. Since the A term is based on $u_{6.1}$, the velocity at 6.1*m* must be used here. Equation (5.2) describes a vertical line appearing on a polar plots as in Figure 4.

For the next case, the wind direction is suddenly changed 90° and subsequently held steady where we have an initially fully developed sea as shown in Figure 5. The response of VPINK is shown in Figure 6 and 7. At each time step the model first calculate the growth then dissipate the wave energy travelling against wind.

Tests of the one dimensional propagation scheme has carried out. Figure 8 shows the propagation of an isolated Gaussian profile with $\mu=0.1$.

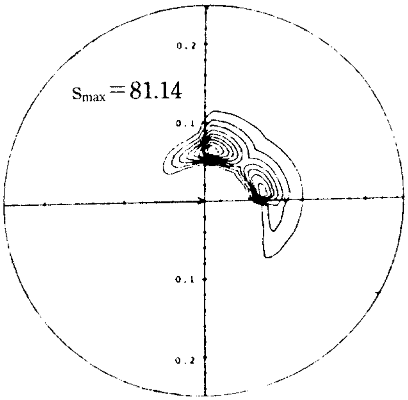

Fig. 6 Contour plot of 2−D spectrum evolution for 90° change of wind directon. T=6 *hours*

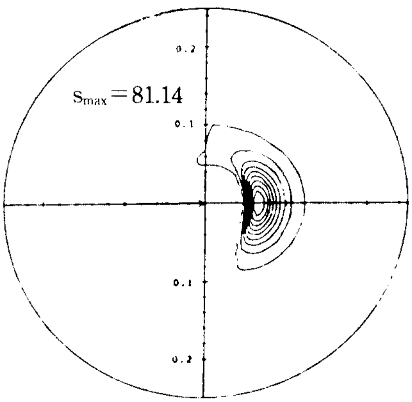

Fig. 7 Contour plot of 2−D spectrum evolution of 90° change of wind direction. T=30 *hours*

Figure 8 a) shows the analytic solution for 200 time steps. Figure 8 b) shows the solution obtained using new integration scheme. Profile shape has been well maintained except a small disturbance in tail. Figure 8 c) is the result calculated from ordinary Lax−Wendroff scheme. It shows poor representation of phase speed and a rapid loss of amplitude in profile.

To test the refraction scheme, the method is applied to the case of wave refraction over a spherical shoal whose bottom topography is shown in Figure 9. Its diameter is 40*m* and water depth of 5*m* at its top set in water of uniform depth 15*m*. The calculation was done for waves with $T_{1/3}=5.1$ *sec* and $H_{1/3}=1m$. Its $60m \times 100m$ geometry is shown in Figure 10. Bretschneider-Mitsuyasu[17] frequency spectrum is adopted whose spectral shape is shown in Figure 11. Mitsuyasu-type spreading function[18] is used which is shown in Figure 12 with $S_{max}=75$. Step sizes are $\Delta x=\Delta y=2.5m$ and $\Delta t=0.4$ *seconds*. It has been determined to satisfy stability of the modified Lax−Wendroff scheme. The wave is a single component ($f=0.17Hz$) travelling up the diagram.

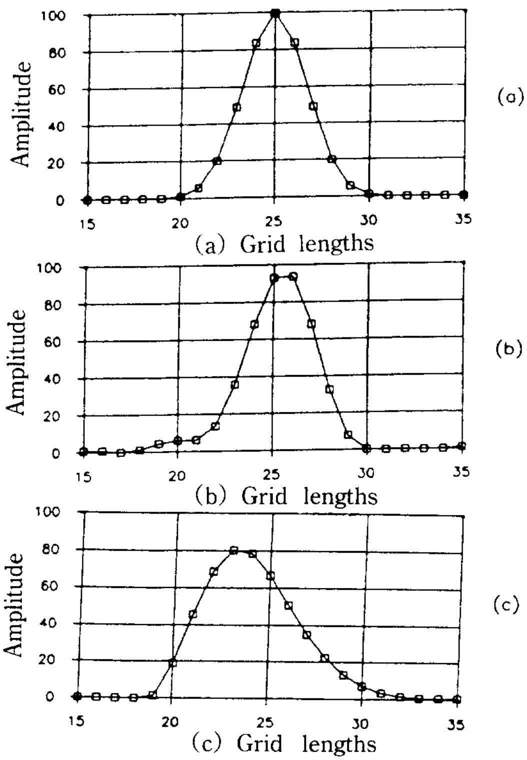

Fig. 8 Gaussain profiles after 200 time steps with $\mu=0.1$

a) analytic,

b) modified Lax-Wendroff scheme,

c) ordinary Lax-Wendroff scheme

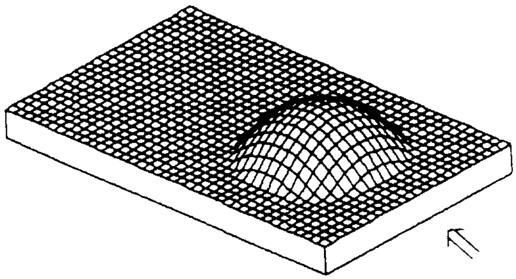

Fig. 9 Bottom topography

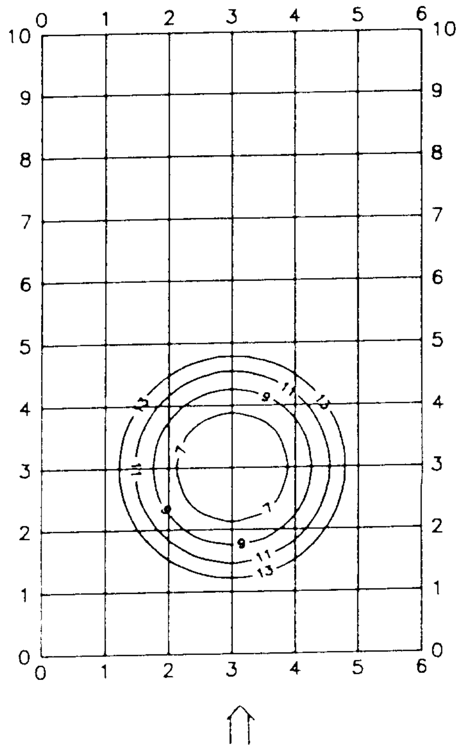

Fig. 10 Wave field geometry and depth contour

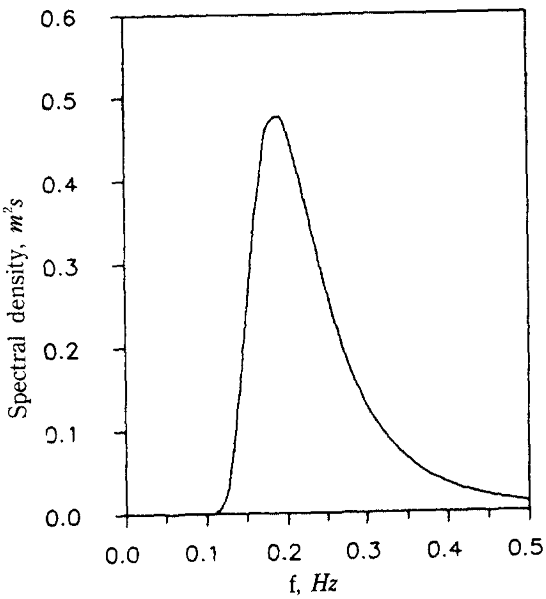

Fig. 11 Bretschneider-Mitsuyasu frequency spectrum

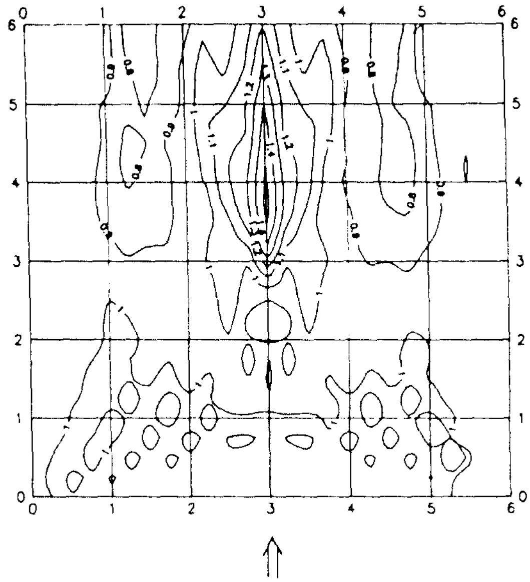

Fig. 13 Contour plot of the wave height ratio over a spherical shoal

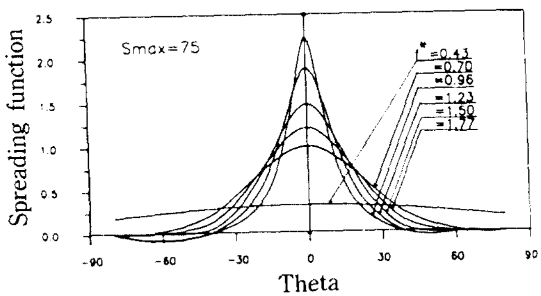

Fig. 12 Mitsuyasu-type spreading function

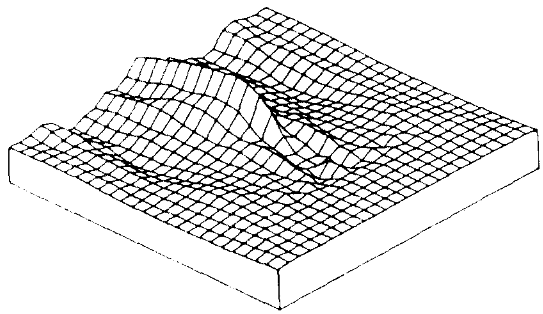

Fig. 14 3−D view of wave height ratio over a spherical shoal

The arrow in the figures indicates the direction of the incoming wave. Figure 13 shows the contour plot of the calculated wave energy. The calculation was done until a stationary state was reached for the entire area. Figure 14 shows the three dimensional view of enhancement of wave energy over the spherical shoal due to the convergence effect of reduced group velocity. The refraction of regular waves over this spherical shoal has been solved by Ito et al.[19] with their numerical technique of wave propagation analysis. The Ito's result of the distribution of wave height is presented in Figure 15. To further investigate the characteristics of the refraction scheme, waves approaching left half of the sea mount is considered. Figure 16 clearly shows a turning of wave energy caused by refraction.

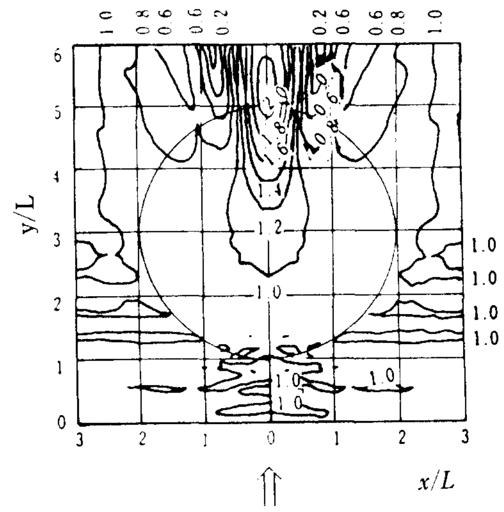

Fig. 15 Distribution of the height ratio of regular waves over a spherical shoal

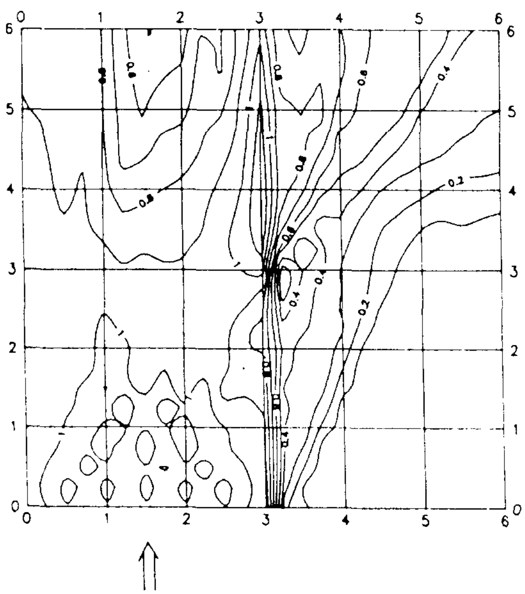

Fig. 16 Contour plot of the wave height ratio. Waves are approaching left half of a spherical shoal.

6. Conclusions

We see that :

1) The proposed model can predict Phillips resonance mechanism with early wave growth test.
2) The proposed model effectively responds to the wind direction change.
3) The modified Lax−Wendroff scheme shows relatively good representation of phase speeds and amplitude.
4) The calculated results of the refraction scheme show similar pattern of wave energy distribution with other author's caculations.

Acknowledgement

The author wishes to express his gratitude to the Korea Science Foundation for its financial support under which this work was carried out.

References

1) Phillips, O.M., "On the Generation of Surface Waves by Turbulent Wind", J. Fluid Mech., Vol 3. pp. 185~204, 1957
2) Neu, W.L. and S.H. Kwon, "A Directional Growth Mechanism for SOWM-Type Wave Model", VPI−AOE−150, 1985
3) Kwon, S.H., "A Directional Growth of Wind Generated Waves", Ph.D Dissertation, Virginia Polytechnic Institute and State University, 1986
4) Neu, W.L. and S.H. Kwon, "A Directional Growth Mechanism for Numerical Wave Model", 20th International Conference on Coastal Engineering in Taipei, Taiwan, 1986
5) Hasselmann, K., "Grungleichugen der Seegangsveroussage", Schiffestechnik, 7, pp. 191, 1960
6) Miles, J. W., "On the Generation of Surface Waves by Shear Flow", Part 1, J. Fluid Mech., 3, pp. 185~204, 1957

7) Miles, J. W., "On the Generation of Surface Waves By Shear Flow", Part 2, J. Fluid Mech., 6, pp. 568~582, 1959
8) Miles, J. W., "On the Generation of Surface Waves By Shear Flow", Part 3, J. Fluid Mech., 6, pp. 583~598, 1959
9) Miles, J. W., "On the Generation of Surface Waves by Shear Flow", Part 4, J. Fluid Mech., 7, pp. 469~478, 1960
10) Phillips, O.M., "The Dynamics of the Upper Ocean", Cambridge University Press, NY, 19 66
11) Pierson, W.J. and Moskowitz, "A Proposed Spectral Form for Fully Developed Sea Based on the Similarity Theory of S.A. Kitaigoroskii", J. Geophys. Res., 69, 5181~5203, 1964
12) Cote, I.J., et al., "The Directional Spectrum of a Wind Generated Sea as Determined by the Stereo Wave Observation Project", Meteo. Pap. Vol. 2, No. 6. New York University, NY, pp. 88, 1960
13) Gadd, A.J., "A Numerical Advection Scheme with Small Phase Errors", Quart. J. R. Met. Soc., Vol. 104, pp. 583~594, 1978
14) Gadd, A.J., "A Split Explicit Integration Scheme for Numerical Weather Prediction", ibid, Vol. 104, pp. 569~582, 1978
15) Gadd, A.J., "Two Refinements of the Split Expicit Integration Scheme", ibid, Vol. 106, pp. 215~220, 1980
16) Golding, B., "A Wave Prediction System for Real-Time Sea State Forecasting", Quart. J.R. Met. Soc., 109, pp. 393~416, 1983
17) Goda, Y., "Random Seas and Design of Maritime Structures", University of Tokyo Press, 1985
18) Mitsuyasu, H. et al., "Observation of the directional Spectrum of Ocean Waves Using a Cloverleaf Buoy", J. Physical Oceanogr., Vol. 5, No. 4, pp. 750~760, 1975
19) Ito, Y., K. Tanimoto, and S. Yamamoto, "Wave Height Distribution in the Region of Ray Crossings-Application of Numerical Analysis Method of Wave Propagation", Rept. Port and Harbor Res. Inst., Vol. 11, No. 3, pp. 88~109, 1972

(Continued to p. 44)